

## Effect of Additives on the Microstructure of Electroplated Tin Films

To cite this article: Yeasir Arafat *et al* 2018 *J. Electrochem. Soc.* **165** D816

View the [article online](#) for updates and enhancements.

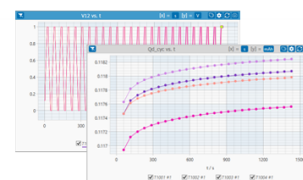
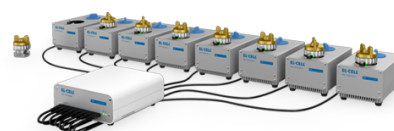
### You may also like

- [Electroless Growth of Size-Controlled Gold Nanoparticles Using Hydroquinone](#)  
Shunsuke Yagi, Naoya Oeda and Chie Kojima
- [Scalable Synthesis and Characterisation of a Liquid 2,3,5,6-tetraallylbenzene-1,4-diol Quinone](#)  
Rune Kjærgaard Groven, Martin Lahn Henriksen, Nihat Ege Sahin *et al.*
- [Aqueous dispersion of hexagonal boron nitride via plasma processing in a hydroquinone solution](#)  
Kenichi Inoue, Taku Goto, Masaki Iida *et al.*

## PAT-Tester-x-8 Potentiostat: Modular Solution for Electrochemical Testing!

 **EL-CELL**<sup>®</sup>  
electrochemical test equipment

- ✓ **Flexible Setup with up to 8 Independent Test Channels!**  
Each with a fully equipped Potentiostat, Galvanostat and EIS!
- ✓ **Perfect Choice for Small-Scale and Special Purpose Testing!**  
Suited for all 3-electrode, optical, dilatometry or force test cells from EL-CELL.
- ✓ **Complete Solution with Extensive Software!**  
Plan, conduct and analyze experiments with EL-Software.
- ✓ **Small Footprint, Easy to Setup and Operate!**  
Usable inside a glove box. Full multi-user, multi-device control via LAN.



Contact us:

☎ +49 40 79012-734

✉ sales@el-cell.com

🌐 www.el-cell.com



## Effect of Additives on the Microstructure of Electroplated Tin Films

Yeasir Arafat,<sup>1,\*</sup> Sujala T. Sultana,<sup>1,a</sup> Indranath Dutta,<sup>1,z</sup> and Rahul Panat <sup>2,z</sup>

<sup>1</sup>School of Mechanical and Materials Engineering, Washington State University, Pullman, Washington 99164, USA

<sup>2</sup>Department of Mechanical Engineering, Carnegie Mellon University, Pittsburgh, Pennsylvania 15213, USA

Electroplated tin films are important for several technologies such as microelectronics, Li-ion batteries, and corrosion-resistant coatings. In this paper, we demonstrate that the microstructure of tin films can be precisely controlled by addition of certain combinations of organic additives to a methanesulfonic acid based electroplating bath. Tin films are deposited on a copper substrate by varying the concentrations of two such additives, namely, hydroquinone and gelatin. The plating process is characterized by linear sweep voltammetry and insights into the resulting microstructure are obtained using imaging by scanning electron microscopy. It is found that the addition of hydroquinone alone results in non-uniform tin films having significant dendrites and does not affect the hydrogen gas evolution during electroplating. The addition of gelatin alone is found to suppress the evolution of hydrogen gas and affects the film nucleation process that controls its grain morphology, but also creates pinholes in the film and sludge in the bath. A combination of the two additives, however, yields a highly uniform grain structure with little to no dendrite formation and a delayed onset of hydrogen gas evolution, which is highly desirable during the electroplating process. Experiments are carried out that show that the mechanism of tin film nucleation and growth during electroplating is altered in the presence of the additives, where gelatin suppresses the tin nucleation rate (thereby controlling the grain size) as well as the formation of large dendrites; while hydroquinone, acting as an antioxidant, prevents pinholes, creates a uniform film, and avoids sludge formation in the presence of gelatin. This work demonstrates a path to control electroplated tin microstructures by varying bath chemistries and process parameters which will prove highly useful to industry.

© 2018 The Electrochemical Society. [DOI: 10.1149/2.0801816jes]

Manuscript submitted October 11, 2018; revised manuscript received November 28, 2018. Published December 20, 2018.

Electroplated tin films are used in several important technological applications such as lead-free electronic interconnects,<sup>1</sup> thermal interface materials,<sup>2</sup> corrosion resistant coatings on structural metals,<sup>3</sup> and Li-ion batteries.<sup>4</sup> Advantages of tin include superior wettability, solderability, high specific capacity for Li storage, as well as a low material and manufacturing cost.<sup>5</sup> Tin and its alloys can be electroplated using solutions containing aqueous fluoroborate, sulfuric acid, methanesulfonic acid (MSA), or phenolsulfonic acid.<sup>6,7</sup> While the electroplating of tin from such acidic electrolytes is possible without additives because of their low activation overpotential, the deposited films from such solutions are found to be coarse, less adherent to the substrate, and having non-uniform and irregular grain sizes and morphologies.<sup>6,8</sup> Further, formation of dendrites during film deposition may often lead to even coarser overall film morphology resulting in mechanical and electrical instability that prohibits their reliable use in electronic devices.<sup>9,10</sup>

In order to obtain desired grain structure and surface finish, several organic additives such as hydroquinone (HQ), gelatin, amine derivatives, glue, thiourea, ethylenediaminetetraacetic acid (EDTA), benzotriazole (BTA) have been evaluated for electroplating of tin and its alloys.<sup>6-8,11-15</sup> The focus of much of the previous work<sup>6-8,11-14</sup> has been to obtain coatings having matte or bright finish without the formation of unwanted dendrites. In spite of this work, there has been little to no emphasis on obtaining a precise control over the microstructure of electroplated tin films using the understanding of the mechanisms of film nucleation and grain growth under different bath chemistries and plating conditions. Note that microstructural control of tin films is highly desirable in several emerging applications as it controls the film mechanical and electrical properties. For example, in the area of wearable electronics, interconnects made up of large equiaxed grain structures are necessary to achieve high ductility and hence stretchability.<sup>16-19</sup> In addition, the electroplating process requires that the film be free from hydrogen embrittlement, and the bath be free of sludges over long periods of time.

Amongst the different additives, HQ (C<sub>6</sub>H<sub>4</sub>(OH)<sub>2</sub>) is an oxidation-inhibitor and when added to the electroplating solution, it significantly lowers the tendency of stannous ions to turn into stannic ions.<sup>8</sup> Further, optimum amounts of added HQ can help suppress hydrogen

evolution during the electroplating process which is one of the critical requirements to form uniform electroplating of metal films.<sup>20</sup> Gelatin, a widely used leveler and grain refiner in metal electroplating processes, has been in use in the industry for several decades.<sup>11</sup> Although there have been studies on the individual effects on these two additives on Sn-Bi alloys,<sup>21,22</sup> very few efforts have been made to identify their combined effects on the electroplating of tin. Furthermore, the dominant mechanisms controlling the nucleation and growth processes during tin electrodeposition in the presence of these two additives are yet to be identified.

The aim of the current work was thus two-fold. First, we aimed to identify the mechanisms of nucleation and growth of electroplated tin films in the presence of two organic additives, HQ and gelatin, to obtain control over film microstructure as a function of the bath chemistry. Second, we aimed to engineer optimum plating conditions that can give rise to higher limiting current density, a delay in the onset of hydrogen evolution, a higher cathodic surface coverage, a dendrite-free film with minimum irregularities, and microstructures consisting of large near-round grains that are desirable to achieve highly ductile tin films that can undergo high deformation without failure.

### Experimental

**Electroplating bath preparation.**—The electroplating solutions were prepared by mixing MSA (assay ≥ 99%) with tin(II) sulfate (assay ≥ 95%) along with HQ (assay ≥ 99.5%) and gelatin (from bovine skin) (all chemicals from Sigma-Aldrich Inc., St. Louis, MO) as additives. Four types of MSA-based solution chemistries were considered, namely, solution with no additives, only HQ as the additive, only gelatin as the additive, and both HQ and gelatin as additives in different ratios. Table I shows the proportion for all the bath constituents for different electroplating conditions. To make the electroplating bath, tin (II) sulfate powder in different proportions was added to MSA solution in a 150 ml beaker under constant stirring conditions followed by an addition of deionized (DI) water (resistivity 18.2 MΩ·cm at 25°C). Although the proportions of the constituents are different for different bath chemistries, the total volume of the solution in each case was maintained at approximately 75 ml. Constant stirring was also applied while adding HQ and/or gelatin to the bath.

A conventional three-electrode cell set-up was used for the voltammetry experiments as shown in the schematic in Fig. 1. An electrochemical workstation (Model CHI660E, serial#A2906,

<sup>a</sup>Present address: Intel Corporation, 5200 NE Elam Young Pkwy, Hillsboro, Oregon 97124, USA.

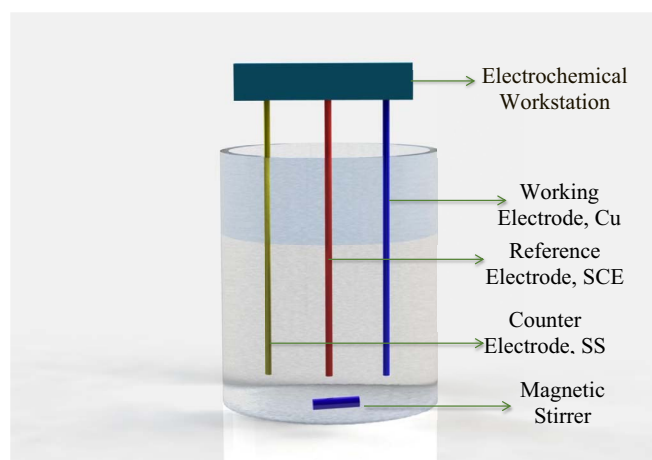
\*Electrochemical Society Student Member.

<sup>z</sup>E-mail: rpanat@andrew.cmu.edu; idutta@wsu.edu

**Table I. Concentrations of chemical constituents of MSA based tin electroplating baths used in this work.**

Solution	Stirring Rate(rpm)	MSA (mL/L)	SnSO <sub>4</sub> (g/L)	HQ(g/L)	Gelatin(g/L)
Ia	200	123.6	20	-	-
Ib	200	123.6	13.33	-	-
Ic	200	123.6	3.33	-	-
IIa	200	123.6	20	6.67	-
IIb	200	123.6	20	5	-
IIc	200	123.6	20	2	-
IIIa	200	123.6	20	-	3.33
IIIb	200	123.6	20	-	2
IIIc	200	123.6	20	-	0.67
IVa	200	123.6	20	6.67	3.33
IVb	200	123.6	20	6.67	2
IVc	200	123.6	20	6.67	0.67
Va	200	123.6	20	5	3.33
Vb	200	123.6	20	5	2
Vc	200	123.6	20	5	0.67
VIa	200	123.6	20	2	3.33
VIb	200	123.6	20	2	2
VIc	200	123.6	20	2	0.67
VI'a	600	123.6	20	2	3.33
VI'b	600	123.6	20	2	2
VI'c	600	123.6	20	2	0.67
VII	200	123.6	30	5	2
VIII	200	123.6	3	5	5.5
IX	200	123.6	30	5	1
X	200	123.6	3	5	1
XI	200	123.6	3	5	1.2

CH Instruments, Austin, TX) interfaced via a software (ver.14.01, CH Instruments, Austin, TX) was used to carry out the Linear Sweep Voltammetry (LSV) experiments with Saturated Calomel Electrode (SCE) as the reference electrode. The working (cathode) and counter (anode) electrodes were Copper (36.86 mm × 6.06 mm) and Stainless Steel (SS) (33 mm × 7.9 mm), respectively. The active surface area exposed to the electrolytic solution was 25.6 mm × 6.06 mm for Cu substrates and 33 mm × 7.9 mm for the SS anode respectively. A magnetic stirrer was used to control the circulation of the charged ions and other chemical constituents in the electroplating solution. For LSV, the working electrode was scanned from 0V vs. SCE to 1.3 V vs. SCE at a rate of 0.01 V/s with a sample interval of 0.001 V, quiet time 2 s, and sensitivity 0.1 (A/V).

**Figure 1.** A Standard three-electrode cell set-up with Saturated Calomel Electrode (SCE) as reference electrode.

The Cu substrates and SS anode were polished using 600 grade SiC papers followed by thorough rinsing with Isopropyl Alcohol (IPA) and DI water before using for voltammetry. The distances between counter electrode, working electrode, and reference electrode were maintained at 10 mm each. A slow stream of pure N<sub>2</sub> gas was applied into the solutions for 10 minutes prior to each LSV experiment. During each LSV experiment, the N<sub>2</sub> gas stream was maintained over the solution surface. This process was adopted to eliminate trapped oxygen from the solution during voltammetry and avoid unwanted oxidation of the constituents.<sup>20</sup>

**Electroplating process and characterization.**—Electroplating of the tin film was done galvanostatically while maintaining 20 mm distance between anode and cathode and using a DC power source (E3611A, Agilent Technologies, Santa Clara, CA). Total time for electroplating was 30 min for each solution at 0.7*i<sub>L</sub>* mA/cm<sup>2</sup> (*i<sub>L</sub>* = limiting current density). From the LSV results, the limiting current densities were determined as midpoints of linear mass-transport controlled regions just before the onset of H<sub>2</sub> evolution. After electrodeposition, each sample was washed with IPA and DI water and air dried at room temperature for 1 hr.

Selected plating solutions were used to electroplate on polished Cu substrates for 10s, 40s, and 150s for a separate set of experiments to understand nucleation and growth mechanism of Sn during electroplating. A constant stirring rate of 200 rpm was maintained for all solutions with exception of solutions VI' (a, b, c) where the rate was kept at 600 rpm (see Table I). The Sn microstructures were studied under a Scanning Electron Microscope (FEI Sirion SEM, FEI Inc., Hillsboro OR) at different magnifications.

## Results and Discussion

**Linear sweep voltammetry.**—Cathodic polarization curves (LSV curves) consisting of the current as a function of the sweep potential (vs. SCE) for bath chemistries I – VI' (Table I) are shown in Fig. 2. For solutions I–VI, the MSA, tin(II) sulfate, HQ and gelatin were varied in different amounts or ratios among the constituent additives within the plating bath. For example, solution I contains only MSA and tin(II) sulfate, solution II contains MSA, tin (II) sulfate and HQ, solution III contains MSA, tin (II) sulfate, and gelatin, whereas all the four constituents were present in different amounts from solution IV to VI. In the case of solution VI', the constituents were identical to solution VI but the stirring rate was increased. In all the cases, the curves show different regions representing different stages of the plating process as described below. At low potentials, the current remains near zero until a certain potential is reached when it starts to rise indicating the beginning of the plating process (i.e. reduction of tin at cathode). Once the plating starts, an activation controlled region is observed where current increases linearly and rapidly with increasing cathodic (i.e., negative) potential, until depletion of the tin ions around the cathode causes the solution to reach a limiting current density, *i<sub>L</sub>*. Activation controlled region appears in the LSV curves due to reduction of Sn ions (charge transfer) that controls the over reaction at this stage. Then an intermediate region is observed which is called mixed controlled region as shown in Fig. 2g where the overall reaction is influenced by both charge transfer and mass transport in the system followed by mass transport region.<sup>23,24</sup> The limiting current density can be predicted by following equation<sup>25,26</sup>

$$i_L = \frac{nFD}{\delta} c_b \quad [1]$$

where, F is Faraday constant, D is diffusion co-efficient,  $\delta$  is the diffusion layer thickness, and *c<sub>b</sub>* is the concentration of tin(II) sulfate. The plating current does not increase further with increasing potential representing the region of concentration polarization. At high potentials, the current starts to increase again primarily due to the undesirable reaction consisting of hydrogen reduction and the evolution of the H<sub>2</sub> gas which can cause film embrittlement. It should be noted that for electroplating tin for practical applications such as interconnects, an

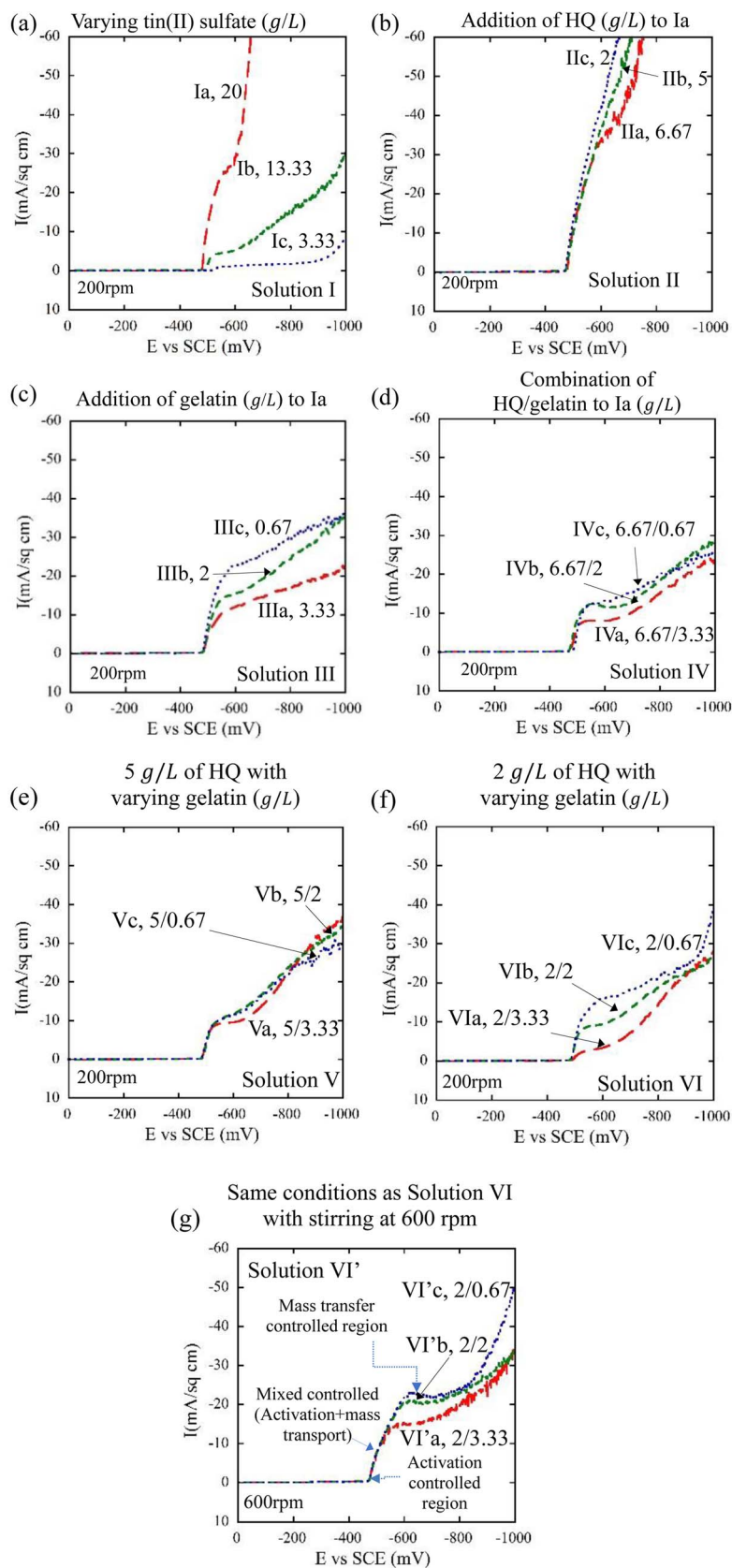


**Figure 2.** Cathodic polarization plots obtained for each solution in Table I. All the solutions were stirred using a constant rpm of 200 except for solution VI' (a, b, c) where rpm of 600 was used for increasing the limiting current density for electrodeposition. The numbers in the bottom right in parentheses denote individual solution numbers from Table I. Fig 2a shows cathodic polarization plots on solutions Ia, Ib, Ic with varying tin(II) sulfate. Fig. 2b shows polarization plot on solutions IIa, IIb, IIc with varying amount of HQ in the solution. Fig. 2c shows similar plots with varying amount of gelatin from solutions IIIa, IIIb, IIIc. From Fig. 2d to Fig. polarization plots are shown from solutions IV to VI' where both HQ and gelatin were varied in the electroplating solutions in various ratios.

optimized process condition is required consisting of a relatively high current density ( $\geq 10\text{ mA/cm}^2$ ) prior to establishment of concentration polarization, as well as a delayed onset of hydrogen reduction.

Figure 2a shows the LSV curves for the solutions Ia, Ib, and Ic (see Table I) where the concentration of tin (II) sulfate was varied (Ia > Ib > Ic). The reduction of tin starts at  $-475\text{ mV vs. SCE}$  for solution Ia which has the higher concentration of tin (II) sulfate ( $c_b$ ) compared to solutions Ib and Ic for which reduction potential shifts toward more negative value of  $-518\text{ mV}$  and  $-540\text{ mV vs. SCE}$ , respectively. The limiting current density changes from  $-26.4\text{ mA/cm}^2$  for solution Ia to  $-1.7\text{ mA/cm}^2$  for solution Ic. However, evolution of hydrogen starts faster in Ia ( $-590\text{ mV vs. SCE}$ ) compared to solutions Ib and Ic where the range for Sn reduction potential without evolution of  $\text{H}_2$  is prolonged due to reduced concentration of tin (II) sulfate. This result clearly shows that increasing the concentration of tin (II) sulfate can increase the plating current and hence the plating rate, but an early evolution of  $\text{H}_2$  gas is expected to lead to a poor deposit quality, as well as possible film embrittlement.<sup>27</sup>

The LSV scans, when varying concentrations of HQ alone was added to solution Ia (Table I, solutions IIa, IIb and IIc), are shown in Fig. 2b. As the HQ (g/L) was added to the solution, the reduction of tin occurred at approximately the same potential ( $-470\text{ mV vs. SCE}$ ). The limiting current densities, however, reduced from  $\sim 50\text{ mA/cm}^2$  to  $\sim 36\text{ mA/cm}^2$  as the HQ concentration increased in the solution. It is important to note that, while the activation region for all solutions (i.e., solutions IIa, IIb and IIc) remained unchanged. Moreover, for solution IIa, the  $\text{H}_2$  evolution started at a higher negative potential ( $\sim 667\text{ mV vs. SCE}$ ) compared to solutions IIb and IIc, which demonstrates that the addition of HQ delays the  $\text{H}_2$  reduction during electrodeposition.

The LSV scans for solutions IIIa, IIIb, IIIc, with varying concentrations of added gelatin to solution Ia, shows initiation of tin reduction at  $-480\text{ mV vs. SCE}$  which is slightly more negative ( $-10\text{ mV}$ ) than solutions with HQ only (Fig. 2b, solutions IIa, IIb, and IIc). For solution IIIa where gelatin is present in the highest concentration, the limiting current density,  $i_L$ , is  $-12\text{ mA/cm}^2$  with hydrogen evolution starting after  $-650\text{ mV vs. SCE}$ . Solution IIb shows a higher  $i_L$  of  $-15\text{ mA/cm}^2$  with wider mass transport control region whereas for solution IIc,  $i_L$  is observed to have the highest value ( $-23\text{ mA/cm}^2$ ) of all three solutions with a mass transport control region longer than in solution IIa but shorter than in solution IIb. Hydrogen reduction potential for solution 2c starts at  $-638\text{ mV vs. SCE}$  which is less negative than for both solutions IIb and IIc.

It is clear from the above results that the addition of HQ or gelatin alone could not give a combination of early onset of Sn reduction with high limiting current density and a delayed hydrogen reduction. The LSV scans of solutions IVa, IVb, IVc, solutions Va, Vb, Vc, and solutions VIa, VIb, VIc which contained a combination of HQ and Gelatin as additives in varying concentrations (see Table I) are shown in Figs. 2d, 2e and 2f respectively. For solutions IVa, IVb, and IVc, where the proportion of HQ to gelatin was varied from 6.67/3.33, 6.67/2, 6.67/0.67, respectively, the tin reduction potentials remained at about  $-470\text{ mV vs. SCE}$ , but  $i_L$  varied as 8, 12 and  $13\text{ mA/cm}^2$ , respectively. For solutions Va, Vb, and Vc and solutions VIa, VIb, VIc the reduction process of tin started at  $-477\text{ mV}$  and  $-480\text{ mV}$  respectively. The limiting current density for the former stayed between  $-9.46\text{ mA/cm}^2$  and  $-6.6\text{ mA/cm}^2$ , while for the latter, it was more distinguishable ( $-3\text{ mA/cm}^2$  to  $-16\text{ mA/cm}^2$ ). The results presented above clearly indicate the effect of a combination of HQ and gelatin on the electrochemical behavior of each solution in terms of reduction potentials of tin and hydrogen, all of them changing with changes in the concentrations of HQ and gelatin. The addition of only HQ was observed to have a relatively weak effect in delaying the onset of hydrogen evolution during cathodic polarization. Gelatin alone had a strong effect on delaying hydrogen reduction after concentration polarization of tin, which suggests adsorption of gelatin on the cathodic surface,<sup>11</sup> and consequent reduction of the number of nucleation sites for tin and hence the peak current density compared to solution II. This is indeed observed in Fig. 2c. However, the addition of both HQ and gelatin in solutions IV, V and VI resulted

in a longer delay in hydrogen evolution. Further, the solutions VI'a, VI'b, and VI'c consisted of HQ/gelatin ratios of 2/0.67, 2/2, 2/3.33, respectively and an increased stirring rate at 600 rpm. As shown in Fig. 2f, the current densities for solutions VI'a, VI'b, VI'c increased to about  $-15$ ,  $-21$  and  $-23\text{ mA/cm}^2$ , respectively; consistent with Eq. 1. Note that the solutions VII, VIII, IX, X, and XI were used to fine tune the microstructure (Figure 5) and their LSV scans are shown in supporting information Fig. S1.

**Film morphology and microstructure.**—From the above section, the addition of a combination of HQ and gelatin in the MSA solution can provide significant improvement in achieving electroplated tin films at high limiting current densities (hence high deposition rate). However, in addition to producing non-porous, un-embrittled films at reasonable deposition rates, it is important to control the film microstructure (e.g., grain size and morphology) for applications where mechanical properties (e.g., ductility and strength) are important. We carried out the electroplating process at 70% of the limiting current density as determined from the plots in Fig. 2 to evaluate the effect of additives on microstructure. Only solutions Ia, IIa, IIIa, and VIa of Table I were selected for these experiments, since they comprise of the solutions without any additives, and with highest amounts of additive concentrations (i.e., HQ alone, or gelatin alone, or with both gelatin and HQ, respectively).

As expected from the significantly different LSV scans seen in Figs. 2a through 2g, the electroplated tin films had remarkably different morphologies and microstructures for different plating chemistries of Table I as shown in Figs. 3a, 3b, 3c, 3d, 3e, 3f, 3g, 3h (plating time of 30 minutes at  $0.7i_L\text{ mA/cm}^2$ ). Figs. 3a and 3b show the film microstructures at the sample center and film morphology at the sample edge, respectively, when no additives were present (solution Ia). The film had a rough morphology and the tin grain sizes and morphologies appeared to be highly irregular (e.g., grain sizes ranging from  $3\text{--}40\text{ }\mu\text{m}$  within a  $120\text{ }\mu\text{m}^2$  area of the film). At the film edges, large dendrites with high aspect ratios were formed, likely due to the presence of higher electric field during electrodeposition. The length of the dendrites was of the order of  $400\text{--}800\text{ }\mu\text{m}$  while the lateral dimension was of the order of  $20\text{--}40\text{ }\mu\text{m}$  (Figs. 3b). We observed, however, that with increased deposition time, the dendritic structures started to lose adhesion with underlying grains of the tin film. Heavy rinsing of the plated film using IPA and DI water was found to be useful in getting rid of only some of the loose dendrites. Note that the formation of these dendrites in any plating process was previously linked with high current density,<sup>28</sup> but in the current experiments it occurred even at low to medium overall current densities, although it is possible that the local current densities were higher due to concentration of the electric field.

Figures 3c and 3d show the film microstructure and morphology when HQ alone was added (solution IIa). The grain size distribution of the deposited tin film in Fig. 3c was narrower than that in Fig. 3a, but still varied from  $5\text{--}20\text{ }\mu\text{m}$ . We also observed dendrites at the edge of the films in Fig. 3d had a shorter length (in the range of  $200\text{--}400\text{ }\mu\text{m}$ ) and a lower density than that in Figs. 3b. When compared to the case with no additives, the film surface texture was found to be more uniform with an improvement in the packing of the grains. Also, addition of HQ prevented sludge formation and preserved the solution for at least 30 days. Preservation and stability of solutions will be discussed in the latter part of the paper.

Figures 3e and 3f show the morphology of electroplated tin films when gelatin alone was added to the plating bath (solution IIIa). Compared to the previous two solutions described above where the grain sizes varied over a rather large range (Figures 3a and 3c), a more uniform distribution of grains was obtained, with grain sizes ranging from  $10$  to  $18\text{ }\mu\text{m}$  ( $\sim 15 \pm 3\text{ }\mu\text{m}$ ). Moreover, the films obtained from these solutions were visibly less rough when compared to the ones obtained from solutions I and II. The grains obtained using gelatin as additive were homogeneously distributed throughout the entire cathode surface. This distribution of grains can be explained by the inhibitory effect of gelatin, which makes the cathode surface less

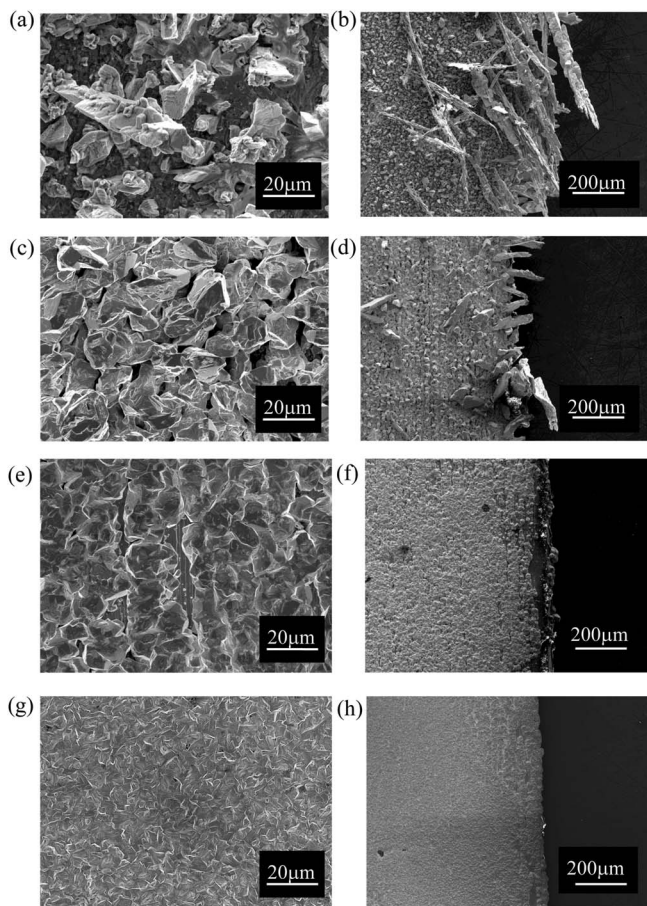


**Figure 3.** Microstructure of the electroplated tin films on Cu substrates at  $0.7i_L$  for: (a, b) plating solution without any additives (solution Ia), (c, d) with HQ only as additive (solution IIa), (e, f) with gelatin only as the additive (solution IIIa), and (g, h) with HQ and gelatin both as additives (VI'a). The images (a, c, e, g) represent microstructure at the sample center (and have the same scale bar as in image (a)), while the images (b, d, f, h) represent the film morphology at the sample edge (and have the same scale bar as in image (b)). The dendrites, when formed, were observed to be at the edges likely due to the higher electric field as a result of edge effect during electrodeposition.

surface-active during the two-step tin-reduction process seen in the voltammetry experiments. Such effect has been described previously for co-plating of Sn-Bi.<sup>21,22</sup> The microstructure in Fig. 3e, however, showed a large numbers of pinholes, and the edges of the films showed non-uniform plating, although the number of dendrites observed was minimal.

Figures 3g and 3h show the morphology of electroplated tin from solution VI'a where HQ and gelatin were present in a ratio of 2:3.33 and the the solution was stirred at 600 rpm (vs a stirring rate of 200 rpm for solutions I to VI). The most distinct feature of the electroplated tin film obtained from this solution was the uniformity of grain sizes and morphology with no overlapping grains and negligible pinhole formation, unlike the previous solutions where multiple regions were found to be without any deposit. SEM images taken at the edges show no sign of dendrite formation, indicating that the solution conducive to depositing a uniform grain morphology. The grain sizes were found to be between 5–7  $\mu\text{m}$  with smooth edges and a minimal variation in grains size and morphology per unit area, resulting in a homogenous tin film. The above results indicate that although the addition of gelatin was seemingly more dominant in grain refining, it is likely that HQ also contributes to the uniformity of grain morphology and size, when both HQ and gelatin are used in combination.

With the realization of uniform pinhole-free dendrite-free tin films shown in Figs. 3g and 3h, it was desired to obtain varying microstructures

by using a combination of HQ and gelatin as additives and varying their ratios and Sn concentration. Figs. 4a, 4b, 4c, and 4d show tin films with markedly different grain morphologies obtained by altering the tin-ion concentration at different HQ to gelatin ratios for solutions VII, VIII, IX, and X in Table I, respectively. Fig. 4a shows large equiaxed grains with the grain size on the order of 3–5  $\mu\text{m}$  with a relatively low variation in grain size (solution VII). Fig. 4b shows a microstructure with nearly square grains with size of the order of 2–3  $\mu\text{m}$  by reducing the tin sulfate concentration and increasing the proportion on gelatin (solution VIII). Fig. 4c shows semi-uniform grains at a grain size of 1–3  $\mu\text{m}$  by reducing the proportion of gelatin (solution X). Lastly, a microstructure with smaller grains and very high aspect ratios (length 2–4  $\mu\text{m}$  and diameter about 500 nm) was obtained by slightly increasing the proportion of gelatin as seen in Fig. 4d (solution XI). It is clear that the microstructure of electroplated tin films is affected by the HQ/gelatin ratios and Sn concentration, which change the nucleation and growth processes, and hence the morphology of the Sn grains.

In order to further change the microstructures using different input parameters, the current densities for solutions VII, VIII, IX, X, and XI were varied and the microstructures were observed under SEM. The morphology of the grains was specified by reporting their height (d) to width (L) ratio which characterizes the aspect ratio. In addition, the grain size was measured by putting a grid of horizontal and vertical lines on an SEM image and reporting the average of the grain size in each direction. Fig. 5 shows the SEM images of microstructures of the solutions VII, VIII, IX, X, and XI at different current densities. The range of the d/L ratio for the microstructures varied from 1–7, while the grain sizes varied from 500 nm to 4  $\mu\text{m}$ .

#### *Mechanisms of film nucleation and growth in the presence of additives.*

—In an effort to understand the effects of each additive on the mechanisms of film nucleation and growth on cathode surfaces, electroplating was carried out with solutions Ia, IIa, IIIa, and VI'a, and the resultant microstructures were observed after deposition for 10s, 40s and 150s. Solutions Ia, IIa, IIIa, and VI'a represent the additive-free electrolyte, electrolyte with HQ alone, electrolyte with gelatin alone, and electrolyte with a combination of HQ and gelatin, respectively. The microstructures at 10s, 40s, and 150s, for solution Ia are shown in Figures 6a, 6b, and 6c respectively. In absence of additives, the nucleation of tin film on Cu cathode was irregular with uneven grain morphologies and sizes. The average grain size ranged from 0.5–5  $\mu\text{m}$ , while the grain morphologies varied from triangular to square to rectangular within the first 10s of the electroplating process Fig 6a. After about 150s, the grains became coarser with large grains growing even larger (up to ~9  $\mu\text{m}$ ) while several smaller grains remaining in the film, which resulted in a highly non-uniform distribution of grains on the cathodic surface. At times up to 150 s, the tin film was dominated by isolated individual grains. For example, at 40 s, in an area of 60  $\times$  40  $\mu\text{m}$ , only 7 isolated grains can be observed larger than about 4  $\mu\text{m}$ . It should be noted that tin can be electrodeposited on a conductive surface with very low activation potential which is largely responsible for immediate reduction of  $\text{Sn}^{++}$  ions at the cathode surface (Fig. 6a). From Figs. 6a, 6b and 6c, it appeared that several smaller grains were unable to attract enough charged tin ions to grow and remained left behind while several other grains grew at a higher rate starting from the early stages resulting in highly uneven texture of the tin films with several areas remaining without any tin present. This is interesting since the larger grains are expected to deplete  $\text{Sn}^{++}$  ions in the electrolyte in their vicinity but this effect may have been overcome by the stronger electric field around the larger grains.

We note that although the tin nucleation was influenced by texture of the Cu surface, the results shown in Figs. 6a, 6b, and 6c can be used to compare nucleation behavior across bath chemistries since their surface preparation was kept constant. Further, the surface morphology used in this study is expected to be representative of that in practical tin plating applications.

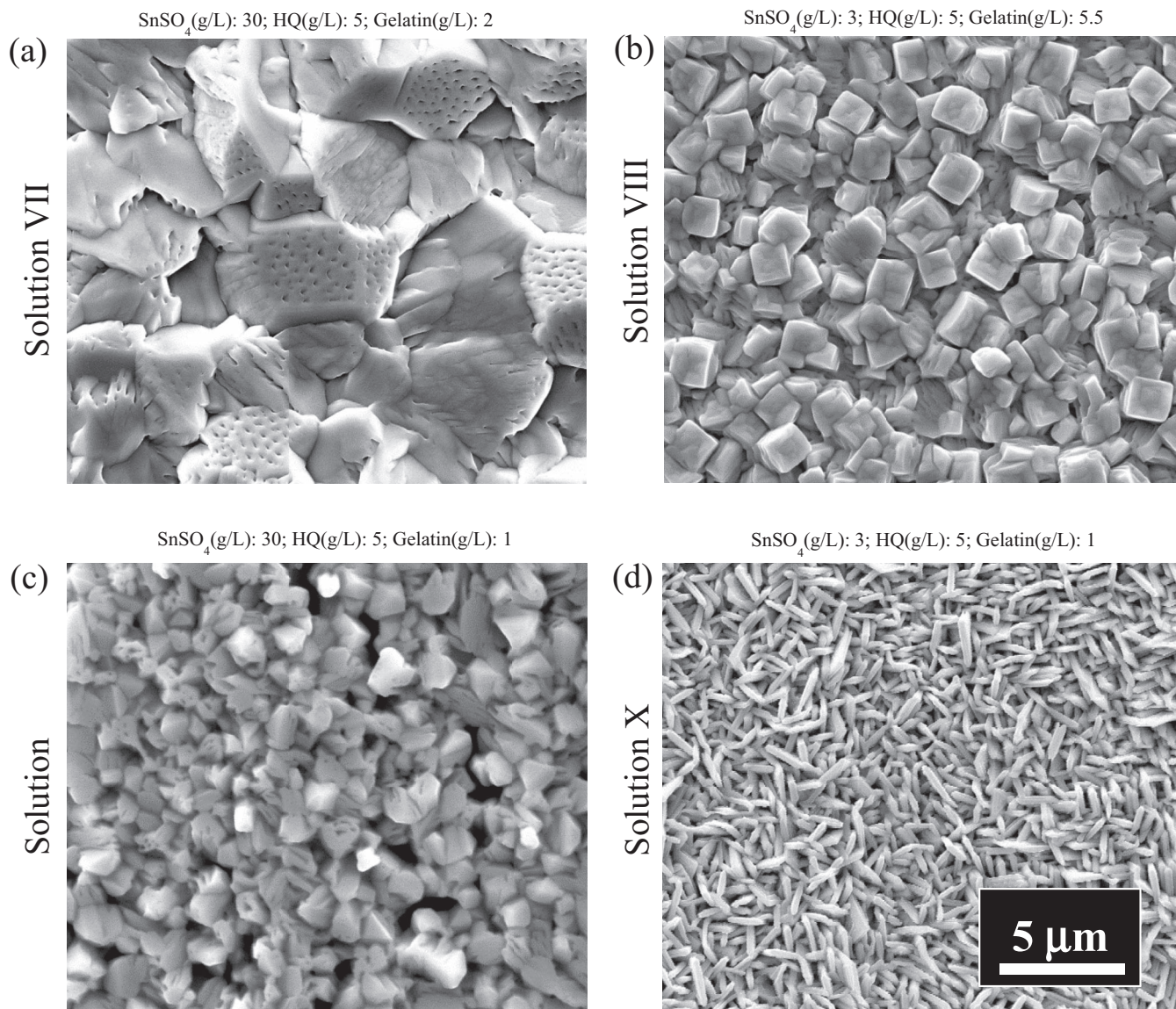


**Figure 4.** Variation in grain morphology and size of electroplated tin from different plating baths with different chemical constituents (different current densities and deposition time 30 mins). The chemical compositions for each image (a-d) of the electroplated solutions are VII, VIII, IX, XI from Table I, respectively. The scale bar is identical for the images in (a-d) and given in (d).

When HQ (6.67 g/L) was added to the solution IIa, the nucleating tin grains were less coarse, more regular, and had an improved grain to grain coalescence (Figs. 6d, 6e, 6f), when compared to that without the additives (Figs. 6a, 6b, 6c). For example, at 10 s, in an area of  $60 \times 40 \mu\text{m}$ , rounded grains of  $0.5\text{--}2 \mu\text{m}$  size in different stages of nucleation can be observed. After 40 s, we observe several coalesced grains that indicated the first signs of film formation. However, after 150s of electroplating (Fig. 6f), the grains grew to about  $6 \mu\text{m}$  in size with visibly less numbers of smaller grains than without any additives (Fig. 6c). However, the surface had regions without tin film that can be potential sites of pinholes we observed in Fig. 3c. The results here indicate that the addition of HQ can alter the electric field and ion concentrations near the cathode such that the grain growth was more uniform and grains were rounded with an improved coalescence compared to that without additives.

Figures 6g, 6h, and 6i show the effect of addition of gelatin (3.33 g/L) alone (i.e. solution IIIa in Table I) to the plating bath on electroplated Sn film at various deposition times. Compared to previous two solutions, the microstructure evolution is completely different in early stages of growth, where we observe smaller grains ranging

from  $20\text{--}700 \text{ nm}$  at a time of 10 s. We note, however, that there were few larger grains with high grain growth rates at sizes ranging from  $1\text{--}4 \mu\text{m}$  which grew to be up to  $13 \mu\text{m}$  after 150 s of electroplating. Apart from few anomalies in grain growth, majority of the electroplated grains were observed to have more uniformly distributed grain size, spherical morphologies, and improved coalescence (Fig. 6).

The comparatively smaller and uniform tin grains observed in the presence of gelatin can be explained by its inhibitory effect (slowing down of tin reduction) which has been found in other systems.<sup>11,12,29</sup> Gelatin is known to combine with metal ions to form charged complexes.<sup>11</sup> For example, in the case of electroplating of Cu, it forms glycine complexes with metal ion such as  $\text{CuGI}^+$ ,  $\text{CuGI}_2$  and  $\text{CuGI}_3^-$  at pH levels ranging from 1.5 to 8.5.<sup>11</sup> In the presence of an acidic environment, gelatin may get decomposed, reducing the probability of presence of complex species in the solution. In the current experiments, the pH level of the solutions ranged from 2–5.5, i.e. within the range mentioned above. It is thus possible that the charged complexes form a film around the cathodic surfaces that inhibits and slows the stannous ( $\text{Sn}^{++}$ ) reduction process. The slowing down of tin reduction reaction is expected to result in more uniformly distributed nucleation

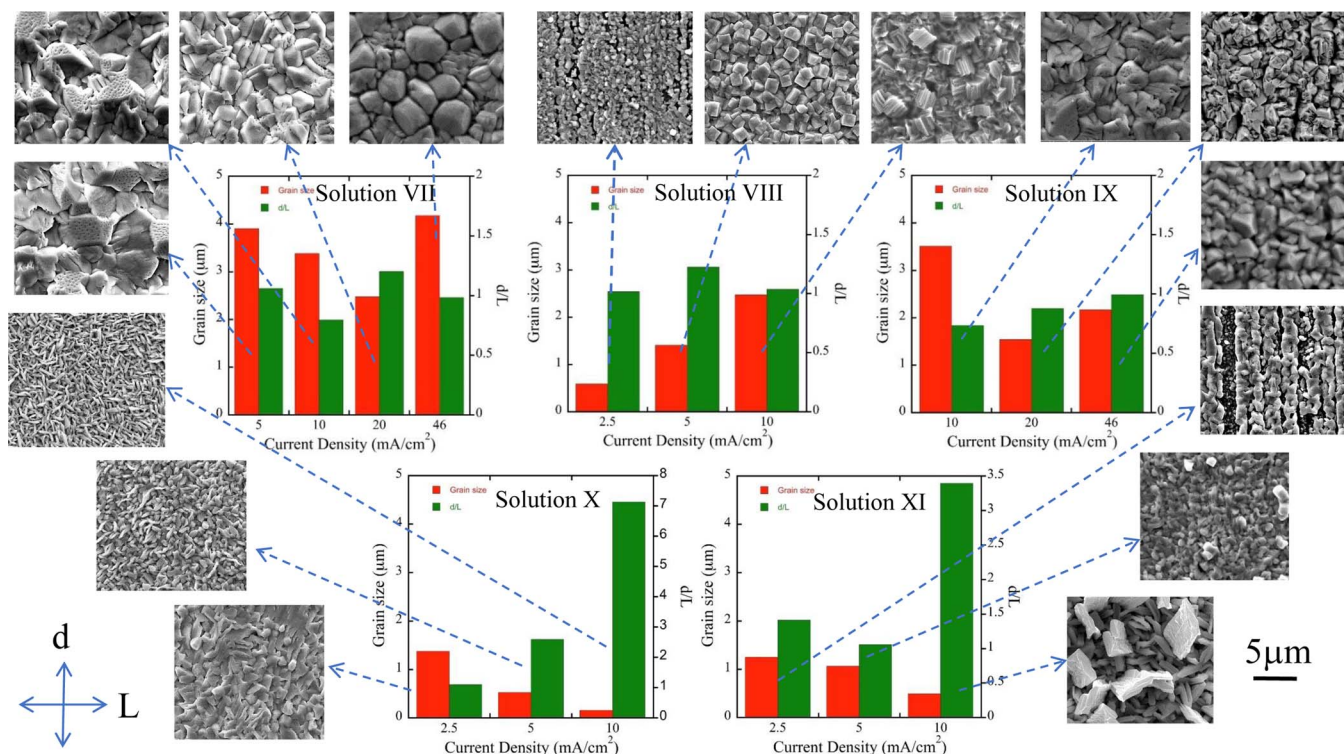


**Figure 5.** Variation in d/L ratio of electroplated tin grains by varying the chemical constituents of the plating solutions.

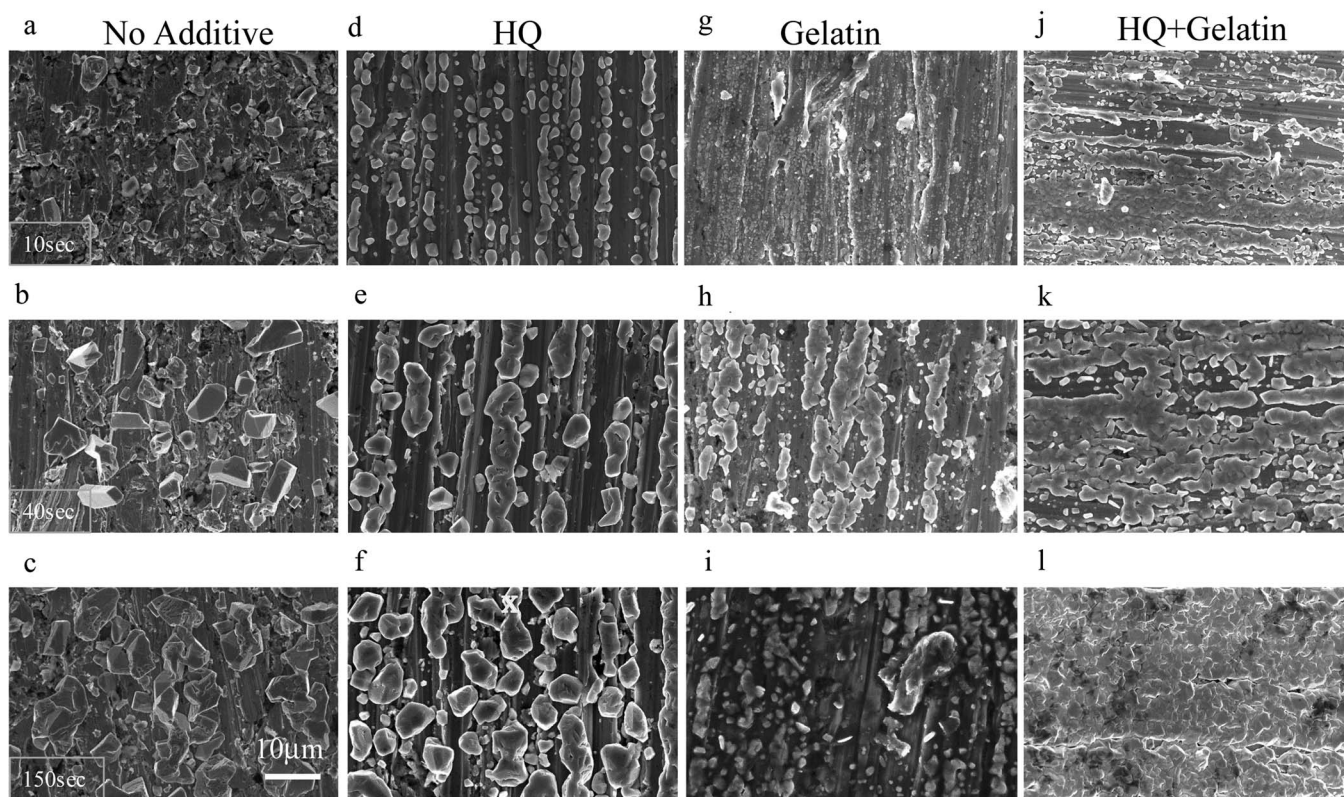


**Figure 6.** Electrodeposition of Sn from different solutions with varying time durations- 10s (first row), 40s (second row) and 150s (third row) with solutions with different chemical compositions- (a-c) no additives present, (d-f) only HQ present as additive, (g-i) only gelatin as additive and (j-l) both HQ and gelatin present from solutions Ia, IIa, IIIa and VI'a respectively. A common scale bar for all the images is shown in (c).



sites at the cathodic surface and a uniform grain growth. The charged complexes can lead to sludge formation and thus deteriorate the electroplating bath. We indeed found this to be the case, where the solution with gelatin alone started to show sludge formation within a few hours of the bath preparation. Another possible explanation of the inhibitory effect of gelatin addition is that gelatin itself can be adsorbed on the cathodic surface during electrodeposition.<sup>11</sup> A measure of adsorption (which also indicates the surface coverage,  $\theta$ ), can be found from the following equation<sup>21</sup>

$$\theta = 1 - \frac{i_{add}}{i} \quad [2]$$

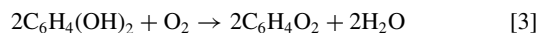
where,  $i$  = current density when gelatin was absent,  $i_{add}$  = current density in presence of gelatin in the solution. For solutions IIIa, IIIb, and IIIc, the current densities found in LSV curves in Fig. 2 indicate that the surface coverage is expected to be 0.15, 0.4 and 0.56, respectively. This indicated a strong adsorption of gelatin on the electrode surface as the concentration of gelatin increased in the plating solution from 0.67, 2, to 3.33 g/L. The nucleation energy for grain formation is expected to reduce which results in a more uniform nucleation rate and the film as stated before.

It should be noted that grain size during electroplating can also be dependent on cathodic overpotential and kinetics of grain growth<sup>30,31</sup> i.e., higher value of cathodic overpotential may lead to nucleation of more grains per unit surface area of the cathode. For obtaining larger grains using the same solutions, increasing current densities can be useful although this will increase the chance of co-reduction of hydrogen gas which may alter mechanical properties of the electrodeposited film i.e., trapped hydrogen within grains can result in brittle films.<sup>27</sup> Since all the electrodeposition experiments were carried out at 30% below each solution's limiting current densities, it is evident that the nucleation and growth of the electroplated Sn films were dominated by the kinetics of the chemical constituents only. Besides, no additional heating of the solution was applied which ensured the prevention of any alteration of the solution's thermodynamic driving force for the tin reduction process.

Figs. 6j, 6k, and 6l show morphology of tin films electroplated at different times when HQ and gelatin were present in the solution (solution VI'a). After 10s of electroplating, the surface of the Cu cathode was observed to have the largest coverage of grains of uniform size of up to ~500nm. This is consistent with that observed in Figs. 3g, and 3h, where the throwing power of this solution was higher than other solutions (Figs. 3a, 3b, 3c, 3d, 3e, 3f). After 150s of electroplating time, the average grain size was observed to be between ~500 nm to 3  $\mu$ m with almost complete coverage. These grains grew up to 5–7  $\mu$ m with no pinholes after 30 mins (Fig. 3g). This is a significant improvement in terms of grain refining and surface coverage, which can be attributed to the increase in nucleation sites per unit area and a uniform nucleation rate and growth. We speculate that gelatin and HQ form complex species in the solution and get adsorbed on the cathodic surface or both additives act individually at the same time without forming any complex to control the kinetics of the overall electroplating process.<sup>11,12</sup> Although it is unclear which of these two factors were dominant, the apparently slower grain growth can indeed be attributed to gelatin's inhibitory effect at current densities lower than  $i_L$  similar to solution III where only gelatin was present as additive. This inhibitory effect of gelatin along with less dominant grain-shaping effect of HQ may have acted together to produce a much refined and uniform electroplated film after 150 s with the largest surface coverage compared to other solutions used in this set of experiments.

**Effect of additives on the stability of electroplating solution.**— Hydroquinone has been used as an additive to protect the electroplating solution from dissolved oxygen and hence it is often called as antioxidant. Without the addition of HQ, the Sn<sup>2+</sup> (Stannous) ions get oxidized to form Sn<sup>4+</sup> (Stannic) precipitates leading toward sludge formation and deterioration of the electroplating bath.<sup>20</sup> Low et al. described the role of HQ as oxygen scavenger where the mecha-

nism was described by the simultaneous occurrence of two chemical reactions in presence of the additive in the solution.<sup>20</sup> First, odorless HQ gets oxidized to form benzoquinone with a redox-couple potential of +699 V vs. Standard Hydrogen Electrode (SHE). Then, the electrons released from the oxidation reaction reduce dissolved oxygen in the electroplating solution to form H<sub>2</sub>O. The complete reaction is therefore



The physical appearance in the absence of HQ was studied in a different set of experiments (solutions Ia, Ib, Ic; IIa, IIb, IIc; IIIa, IIIb, IIIc) where the solutions without HQ formed sludge within less than 6 hours and turned from colorless to yellow because of the formation of tin oxide precipitates. Addition of gelatin alone in the solution deteriorated within less than 24 hours and the color turned dark brown. Solutions IV, V, VI where HQ and gelatin were both present at different ratios were visibly transparent up to 3 months before forming sludge and precipitates. The results here indicate that addition of HQ alone can limit sludge formation and the solution can be preserved for longer periods of time which is critical for industrial applications and was directly observed in the current work.

## Conclusions

This work provides several key insights into the effect of organic additives of HQ and gelatin on the microstructure of electroplated tin films. We have demonstrated a method to produce uniform pinhole-free electroplated tin films such that the film microstructure can be precisely controlled by the electroplating bath constituents. Further, we show that the mechanisms of tin nucleation and growth are altered in the presence of a combination of HQ and gelatin as the additives. The additives create a uniform chemical barrier to the tin nucleation, thereby slowing down the nucleation rate and allowing the film to have a uniform microstructure. Further, the additives alter the cathodic polarization curves and cause a delay in hydrogen reduction in the solution, thereby providing a wide window for tin reduction in combination with a reduced risk of hydrogen embrittlement. Finally, the additives alter the chemical reactions that prevent formation of sludges in the solution which preserves the plating bath for longer periods of time. The above work can be used to create tin films with tailored properties for specific applications such as microelectronics, energy storage, and corrosion resistant coatings.

## Acknowledgment

The authors thankfully acknowledge the assistance of Prof. Yuehe Lin and Shao Feng at WSU with carrying out voltammetry experiments.

## ORCID

Rahul Panat  <https://orcid.org/0000-0002-4824-2936>

## References

1. M. Abtew and G. Selvaduray, *Materials Science and Engineering: R: Reports*, **27**, 95 (2000).
2. B. Feng, F. Faruque, P. Bao, A.-T. Chien, S. Kumar, and G. Peterson, *Applied Physics Letters*, **102**, 093105 (2013).
3. E. Morgan, *Tinplate & Modern Canmaking Technology*, Elsevier (2016).
4. Y. Idota, T. Kubota, A. Matsufuji, Y. Maekawa, and T. Miyasaka, *Science*, **276**, 1395 (1997).
5. H. R. Kotadia, P. D. Howes, and S. H. Mannan, *Microelectronics Reliability*, **54**, 1253 (2014).
6. F.-X. Xiao, X.-N. Shen, F.-Z. Ren, and A. A. Volinsky, *Int. J. Miner Metall Mater*, **20**, 472 (2013).
7. A. Collazo, R. Figueroa, X. Nóvoa, and C. Pérez, *Surface and Coatings Technology*, **280**, 8 (2015).
8. Allen J. Bard, Larry R. Faulkner, Johna Leddy, and Cynthia G. Zoski, *Electrochemical methods: fundamentals and applications*, **2**, New York: wiley, (1980).
9. D. Minzari, F. B. Grummen, M. S. Jellesen, P. Møller, and R. Ambat, *Corrosion Science*, **53**, 1659 (2011).

10. F. Weinberg and B. Chalmers, *Canadian Journal of Physics*, **30**, 488 (1952).
11. C. Meudre, L. Ricq, J.-Y. Hihn, V. Moutarlier, A. Monnin, and O. Heintz, *Surface and Coatings Technology*, **252**, 93 (2014).
12. Y. Goh, A. Haseeb, and M. F. M. Sabri, *Electrochimica Acta*, **90**, 265 (2013).
13. Y. Nakamura, N. Kaneko, and H. Nezu, *Journal of applied electrochemistry*, **24**, 569 (1994).
14. L. E. Stout and A. Erspamer, *Transactions of The Electrochemical Society*, **68**, 483 (1935).
15. A. Sharma, S. Das, and K. Das, in *Electroplating of Nanostructures*, M. Aliofkhaezrai Editor, InTech (2015).
16. J. A. del Valle, F. Carreño, and O. A. Ruano, *Acta Materialia*, **54**, 4247 (2006).
17. A. Lasalmonie and J. L. Strudel, *J. Mater Sci*, **21**, (1837).
18. S. Nakahara, Y. Okinaka, and H. K. Straschil, *J. Electrochem. Soc.*, **136**, 1120 (1989).
19. E. M. Schulson, T. P. Weihs, D. V. Viens, and I. Baker, *Acta Metallurgica*, **33**, 1587 (1985).
20. C. T. J. Low and F. C. Walsh, *Electrochimica Acta*, **53**, 5280 (2008).
21. Y. Goh, A. S. M. A. Haseeb, and M. F. M. Sabri, *Electrochimica Acta*, **90**, 265 (2013).
22. Y. Goh and A. Haseeb, *J. Mater Sci*, **51**, 5823 (2016).
23. C. Ponce-de-Leon, C. Low, G. Kear, and F. Walsh, *Journal of Applied Electrochemistry*, **37**, 1261 (2007).
24. D. Pletcher and F. Walsh, New York (1982).
25. M. Schlesinger and M. Paunovic, *Modern Electroplating*, 5th Edition, Wiley (2014).
26. A. J. Bard, L. R. Faulkner, J. Leddy, and C. G. Zoski, *Electrochemical methods: fundamentals and applications*. Vol. 2. New York: Wiley (1980).
27. A. Sharma, Y. Jang, and J. Jung, *Surface Engineering*, **31**, 458 (2015).
28. H. Chiew Ying, A. S. M. A. Haseeb, Y. Goh, F. Lee Seen, and p. 286 in (2012).
29. V. R. Rao and A. C. Hegde, *Metall and Materi Trans B*, **44**, 1236 (2013).
30. S. Kim, K. Kim, C. Park, and H. Kwon, *Journal of Applied Electrochemistry*, **32**, 1247 (2002).
31. L. Guo and P. C. Searson, *Electrochimica Acta*, **55**, 4086 (2010).